Effect of Mn/Ni ratio variation on microstructure of W–Ni–Mn alloy

S. M. Zahraee[1]*, H. Arabi[2], M. T. Salehi[2] and M. Tamizifar[2]

Tungsten heavy alloys (WHA) such as W–Ni–Cu and W–Ni–Fe are usually used as kinetic energy penetrators (KEP). However, the amount of penetration of these alloys is not sufficient due to their mushrooming effect that occurs as they impact their targets. On the other hand, KEP made of depleted uranium (DU) in spite of their excellent penetrating properties are not a very good substitute for WHA due to their environmental problems. Therefore, in order to increase the penetration depth of WHA penetrators, a new brand of WHA namely W–Ni–Mn alloys have been developed. The present paper deals with the microstructural improvement of such an alloy system, so that it can provide a potential candidate material to be used as KEP, having sufficient penetration depth. For developing this material, various ratios of Mn/Ni powder were mixed with 90 wt-% pure tungsten powder before compaction and sintering in order to investigate the amount of solubility of W in Ni–Mn matrix. In addition to study the effect of this ratio on the re precipitation and growth of W particles within the matrix after being subjected to sintering process, the results of the present study indicated that the grain refinement of W grains is possible by addition of Mn to W–Ni heavy alloys, so that the higher the amount of Mn/Ni ratio up to certain amount, the smaller will become the W grain size after sintering process. Worth mentioning that according to the results obtained by other researchers for WHA penetrators, the finer W grain size, the deeper the penetration of KEP would be. In addition, the results of the present study show that by selecting a suitable sintering cycle, one may obtain a dense microstructure having a density of ~100%, i.e. 99·6%.

Keywords: Tungsten heavy alloy, W–Ni–Mn system, Depleted uranium, Mn/Ni ratio

Introduction

Tungsten heavy alloys (WHA) are a kind of metal matrix composite materials consisted of two phases of tungsten particles in a relatively low melting temperature matrix. The matrix is generally composed of Ni and a transition element, such as Fe, Cu and Co. They are fabricated by liquid phase sintering (LPS).[1] Owing to their high density and high strength associated with the bcc tungsten phase and their high ductility due to their fcc matrix, these alloys are used in applications such as radiation shielding, counterbalance, vibrational damping devices as well as kinetic energy penetrators (KEP).[2]

It has been reported[3–5] that other high density materials such as depleted uranium (DU) are being used as KEP in limited form to contain sever crises in some region of the world such as Persian Gulf area, but due to their dangerous environmental side effects the use of these type of penetrators are under increasing criticism world wide.[6,7] On the other hand, DU penetrators have a determining effect on the battle field, as these types of KEP can penetrate effectively into the targets due to their self sharpening effect. But, bearing in mind that DU penetrators have been used several times during the past battles,[3–7] one would be very naive to believe that those who had these types of penetrators in their possession did not use it again in order to make their own ends meet. Thus, this mater makes the production of a type of penetrator with similar properties of DU penetrators without having their dangerous environmental side effects very attractive.

It has been reported[8,9] that penetrators made of WHA which consist of mainly W–Ni and small amount of other elements such as Cu, Co, Fe have good mechanical properties at low strain rates, but their penetration performances are inferior to DU penetrators. This inferiority is said to be[2,8] associated with their low tendency for formation of adiabatic shear bands (ASB) which cause mushrooming effect when they hit the target, hence less penetration.[2,9] These bands are reported[8,9] to be the main factor for induction of self sharpening effect in KEP. Schematic mushrooming effect in WHA and self-sharpening effect in DU penetrators can be seen in Fig. 1.

[1]Advance Materials Center, Iranian Research Organization for Science and Technology (IROST) Tehran, 15819 Iran
[2]Department of Metallurgy and Materials Engineering, Iran University of Science & Technology (IUST) Narmak, Tehran, 16846 Iran

*Corresponding author, email smzahraee@irost.org

Published by Maney on behalf of the Institute
Received 2 December 2006; accepted 3 February 2007
DOI 10.1179/174329007X204885

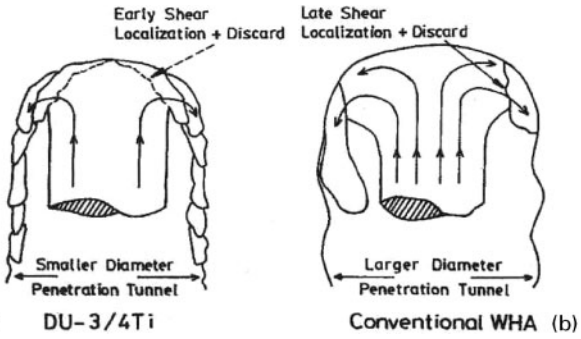

1 Schematic diagrams of *a* self-sharpening effect in DU and *b* mushrooming effect in WHA penetrators[2]

It has been found[10,11] that factors increasing ASB are: low values of thermal conductivity, specific heat, density and strain hardening rate and high values of shear yields stress, thermal softening rate and hardness as well as smaller tungsten grains within the matrix.

Among the influencing factors on the formation of ASB, thermal conductivity and tungsten grain size have been reported[12,13] to have the most important role. This is due to the adiabatic condition which is directly related to thermal conduction through the material and smaller tungsten grain size that favour the propagation of the shear bands.

The thermal conductivity of Mn is very low, i.e. 1/10 of that of Fe, therefore it is said[10] that the addition of Mn instead of Fe to the conventional heavy alloy system promotes the formation of ASB. Table 1 shows some properties of Mn in comparison with Fe, Cu and DU.

Since no published phase diagram was available for W–Mn binary system, it was not possible to predict the amount of tungsten that would be taken in solution during LPS of W–Ni–Mn alloy in this research. However, the amount of tungsten that can be taken in solution within the Ni–Mn matrix during LPS of W–Ni–Mn alloy has been reported to be very limited,[14] so the growth of tungsten grains by Ostwald ripening mechanism within a matrix having a large amount of Mn is expected not to be very much. In other words, since the amount of tungsten within the solid solution of Ni–Mn matrix is very low and each grain of W is surrounded by a film of Ni–Mn matrix, the amount of W atoms required for growth of W particles by the above mentioned mechanism is very limited; hence one can observe smaller W grain in W–Ni–Mn alloys.

Considering the above discussion and the fact that the amount of publication about the effect of Mn on various properties of W heavy alloys is very limited, it was found useful to investigate the effect of Mn on the microstructure and mechanical properties of W heavy alloys.

The present study intends to investigate the effects of Mn addition to a W–Ni alloy in order to monitor the microstructure changes, and to find the best condition which leads to formation of smaller W grains, hence better self-sharpening effect.

Table 2 Characteristics of powders used in this research

Characteristics	Powder W	Ni	Mn
Purity, %	99·99	99·99	99·99
Mean particle size, μm	4–5	<5	<5
Apparent density, g cm^{-3}	2·8	2·25	2·41
Tap density, g cm^{-3}	5	3·3	3·4

Experimental

The characteristics of the powders used in the present study are shown in Table 2 and their morphologies are shown in Fig. 2.

Several samples with the same amount of tungsten, i.e. 90 wt-%, but different amounts of Mn/Ni ratio were produced by powder metallurgy technique. The Mn/Ni ratio used in this research were 1/9, 2/8, 3/7, 4/6, 5/5, 6/4 and 8/2. The powders weighed and mixed in a turbula mixer for 45 min without using any binder. The mixed powders were sealed in elastomer bags and compacted by a cold isostatic press (CIP) at 200 MPa. Then the compacted green samples were subjected to LPS process. Sintering was performed in a horizontal tube furnace under controlled atmosphere, using very high purity argon and hydrogen gases. The purity of argon and hydrogen gases used in the present work was 99·999% and the due point of dry hydrogen gas used was −60°C.

The sintering cycle consisted of heating up to reduction temperature under argon gas, then the atmosphere was changed to dry hydrogen, holding it at reduction temperature for 90 min and finally heating it up to the sintering temperature and holding at this temperature for 60 min.The heating rate used up to reduction temperature was 10°C min^{-1} and from reduction temperature to sintering temperature was 5°C min^{-1}. The reduction temperature used varied from 1000 to 1300°C depending on the compositions of the alloys used.

Sintering temperature for each composition varied between 1050 and 1500°C depended on Mn/Ni ratio. This temperature was chosen to be ~100°C higher than that of the liquidus temperature indicated in the Mn–Ni binary phase diagram,[15] as shown in Fig. 3.

The cooling rate was 5°C min^{-1} for the first 200°C below sintering temperature and then down to 300°C was 25°C min^{-1}. Finally the furnace was switched off at 300°C, so that the samples were gradually cooled down to room temperature. Figure 4 shows a typical sintering cycle adapted for sintering the samples in the present study.

After sintering, the cylindrical specimens, they were bisected perpendicular to the longitudinal direction of

Table 1 Physical properties of Mn in comparison with some other elements

Properties	Element W	Ni	Cu	Fe	U	Mn
Thermal conductivity, W m^{-1} K^{-1}	170	88·5	400	78·2	28	7·8
Melting point, °C	3410	1455	1085	1538	1132	1246
Density, g cm^{-3}	19·3	8·9	8·92	7·87	19	7·43
Specific heat, J kg^{-1} K^{-1}	138	452	380	456	117	486

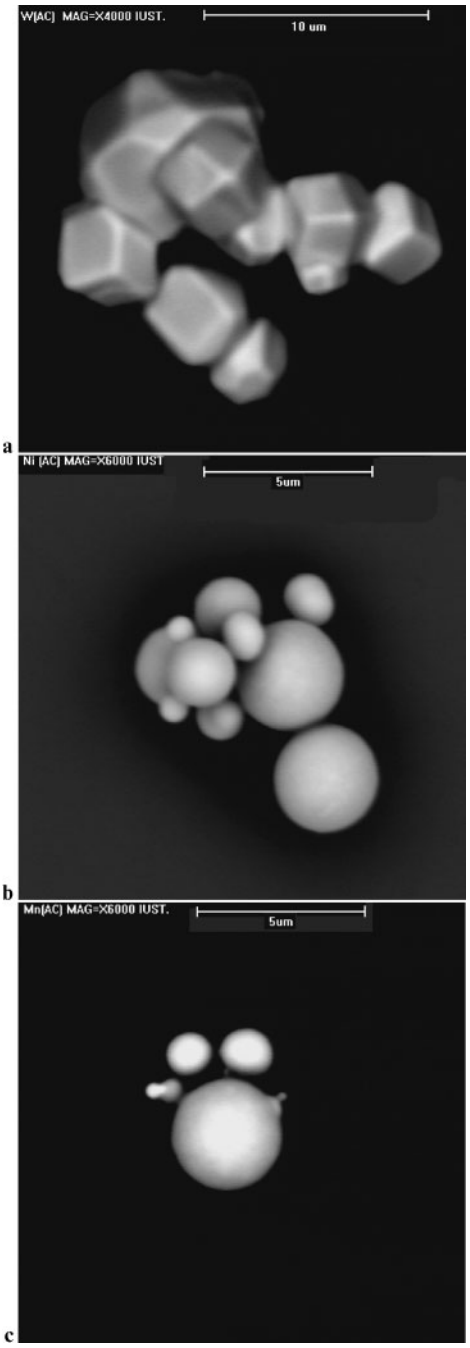

2 Sizes and morphologies of powder used *a* W, *b* Ni and *c* Mn powders

the samples by a diamond saw. The longitudinal sections were then mounted and prepared for metallographic study. These samples were etched in Muorakami's solution for a period of 30 s before studying their microstructure by light and scanning electron microscopes. Tungsten grains sizes for various samples having different Mn/Ni ratios were determined by an image analyser (IA). The chemical compositions of the matrixes were established by energy dispersive spectroscopy (EDS) technique. The average value of each matrix composition was taken from five different positions within the Ni–Mn matrix.

Results and discussion

It should be noted that, the initial constituent powders have invariably oxide on their surfaces. If these oxides are not reduced, they will restrict densification during sintering. Therefore, before LPS, these oxides must be reduced. The LPS temperature of the alloys depends on their compositions. The minimum temperature for formation of liquid phase for the composition 90W–4Ni–6Mn used in this research is ~1030°C (*see* Fig. 3). Therefore, it was decided to use a reduction temperature of at least 1000°C, as this temperature is below the liquid formation temperature.

According to the oxidation–reduction equilibrium diagram[16] shown in Fig. 5, for MnO reduction, the due point of dry hydrogen at this temperature (1000°C) is −60°C. It should be noted that Mn is more prone to oxidation than W and Mi. In other word, reduction of MnO at due point less than −60°C (e.g. −30°C) at 1000°C is not possible thermodynamically. Therefore, on the base of this argument a dry hydrogen gas was chosen with a due point of −60°C to be used for reduction of the compacts at 1000°C or more. In other words, for the alloys having their liquid formation temperature more than 1030°C, their reduction temperature can be increased providing they do not exceed their minimum liquid formation temperature. When higher temperature for reduction used, with a hydrogen gas having a due point of −60°C or more (e.g. −70°C) a better reduction condition is established.

The average grain size of tungsten particle together with the average values of tungsten solubility in Mn–Ni matrix as a function of Mn/Ni ratio is shown in Fig. 6. These results show that by increasing Mn/Ni ratio the amount of solubility of W in the matrix decreased. These results were also confirmed by the EDS profiles obtained from matrix of the samples having Mn/Ni=1/9 and Mn/Ni=8/2 as shown in Fig. 7.

This effect was expected as tungsten has no solubility in manganese, so its solubility in the matrix should decrease as Mn content increased. This resulted to smaller tungsten grains as shown in Fig. 8. A sharp increase in solubility of tungsten in the matrix occurred below the ratio of Mn/Ni=5/5 as shown in Fig. 6. When the amount of Mn increased within the matrix, it seems that the extra Mn prevented very effectively the coarsening of the W grains due to reduction of solubility of W in the matrix.

As the Mn/Ni ratio decreased (*see* Fig. 9), the grains of tungsten became more spherical, indicating an increasing dissolution of tungsten from the sharp edges of large W particles as well as dissolution of smaller W particles to the surrounding molten matrix. One should note that when the sintering process continues, the matrix becomes gradually saturated from tungsten and subsequently reprecipitation of W on to the coarse W grains occurs, according to solution–reprecipitation process.[17] Therefore, the sintering time should be optimised. If the sintering time exceeds 60 min, a great amount of grain growth occurs and the growth of trapped vapour within the structure will happen. These cause a decrease in density and degradation of mechanical properties. On the other hand, when the sintering time is <60 min, the rearrangement of W particles within the matrix does not occur properly, the contiguity will be high, and also solution of tungsten in the matrix will not be sufficient for reprecipitation of tungsten. These phenomena once more result in an unsound microstructure with inferior mechanical properties.

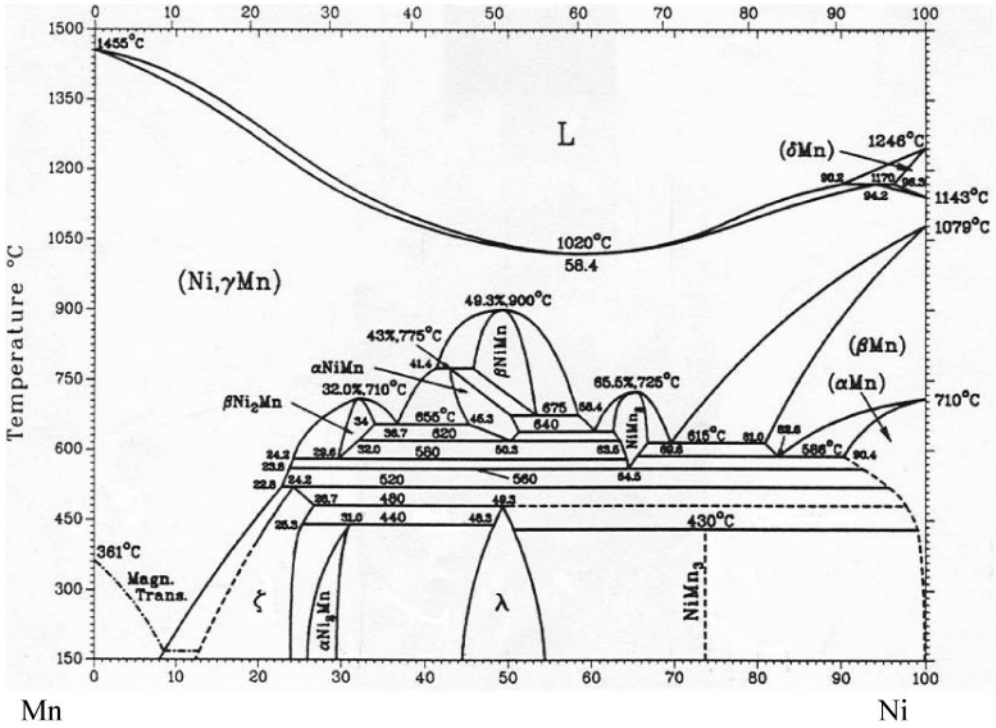

3 Binary phase diagram of Ni–Mn (Ref. 15)

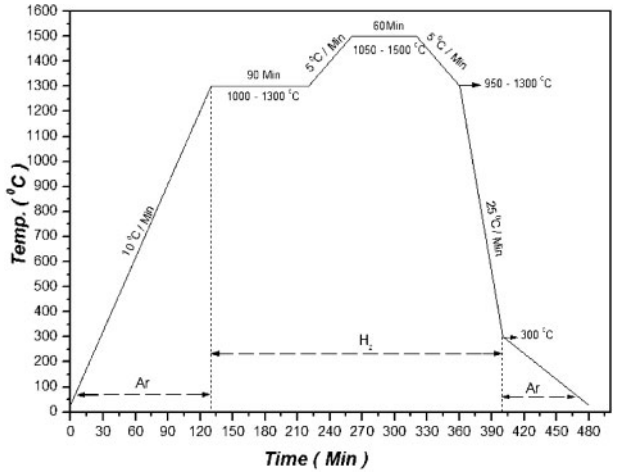

4 Typical sintering cycle used for 90W–9Ni–Mn

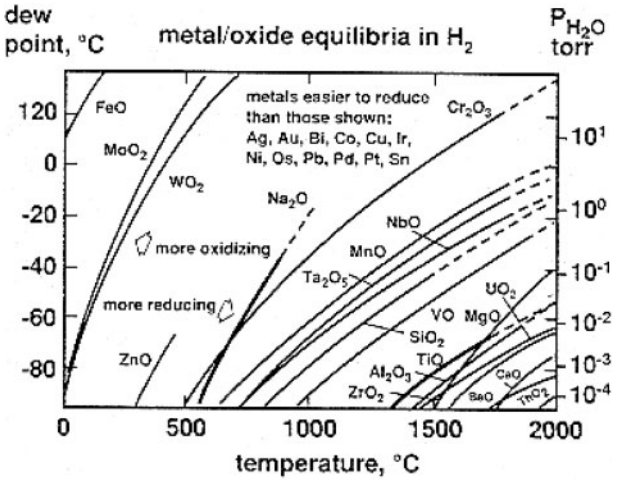

5 Oxidation–reduction equilibrium in terms of temperature dew point for several metals and oxides[16]

Therefore, 60 min was in fact the optimised sintering time chosen in the present work.

Although sintering is not an equilibrium process, one may use equilibrium phase diagrams to predict the formation of phases and select other process variables.[18] Therefore, since neither W–Mn binary phase diagram nor W–Ni–Mn ternary phase diagram was available, Mn–Ni binary phase diagram shown in Fig. 3 was used for predicting liquid formation temperature in this research. Then, the sintering temperature was chosen approximately 100°C more than liquid formation temperature. The chosen sintering cycle together with the compaction process used, i.e. CIP, resulted to a sintered density 99·6% of theoretical density.

The coarsening of tungsten grain size within Ni–Mn matrix in comparison to tungsten within Ni–Fe matrix[2] for similar sintering time (60 min) was much smaller as shown in Fig. 10.

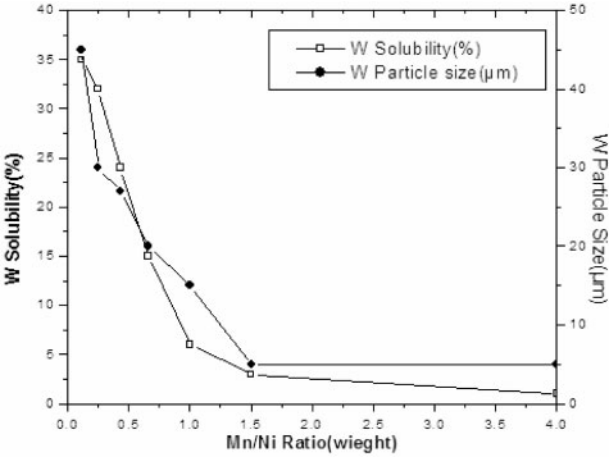

6 Tungsten solubility and particle sizes via Mn/Ni ratio

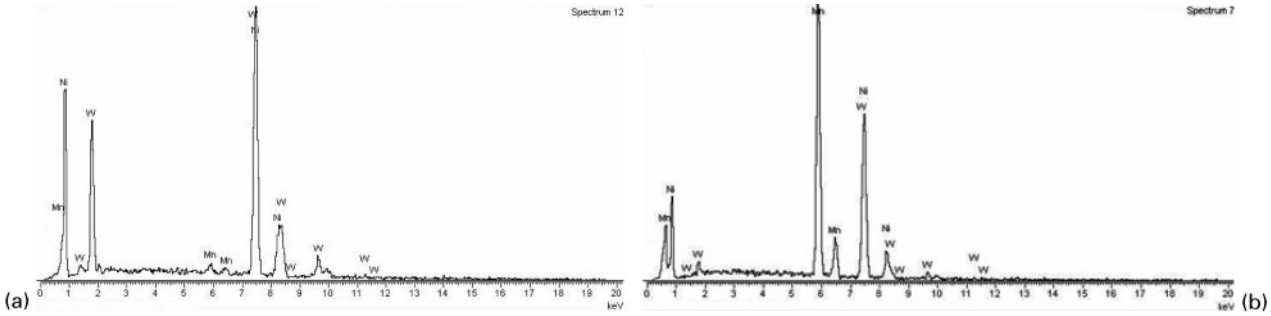

7 EDS Profiles of W–Ni–Mn matrix *a* Mn/Ni=1/9; *b* Mn/Ni=8/2

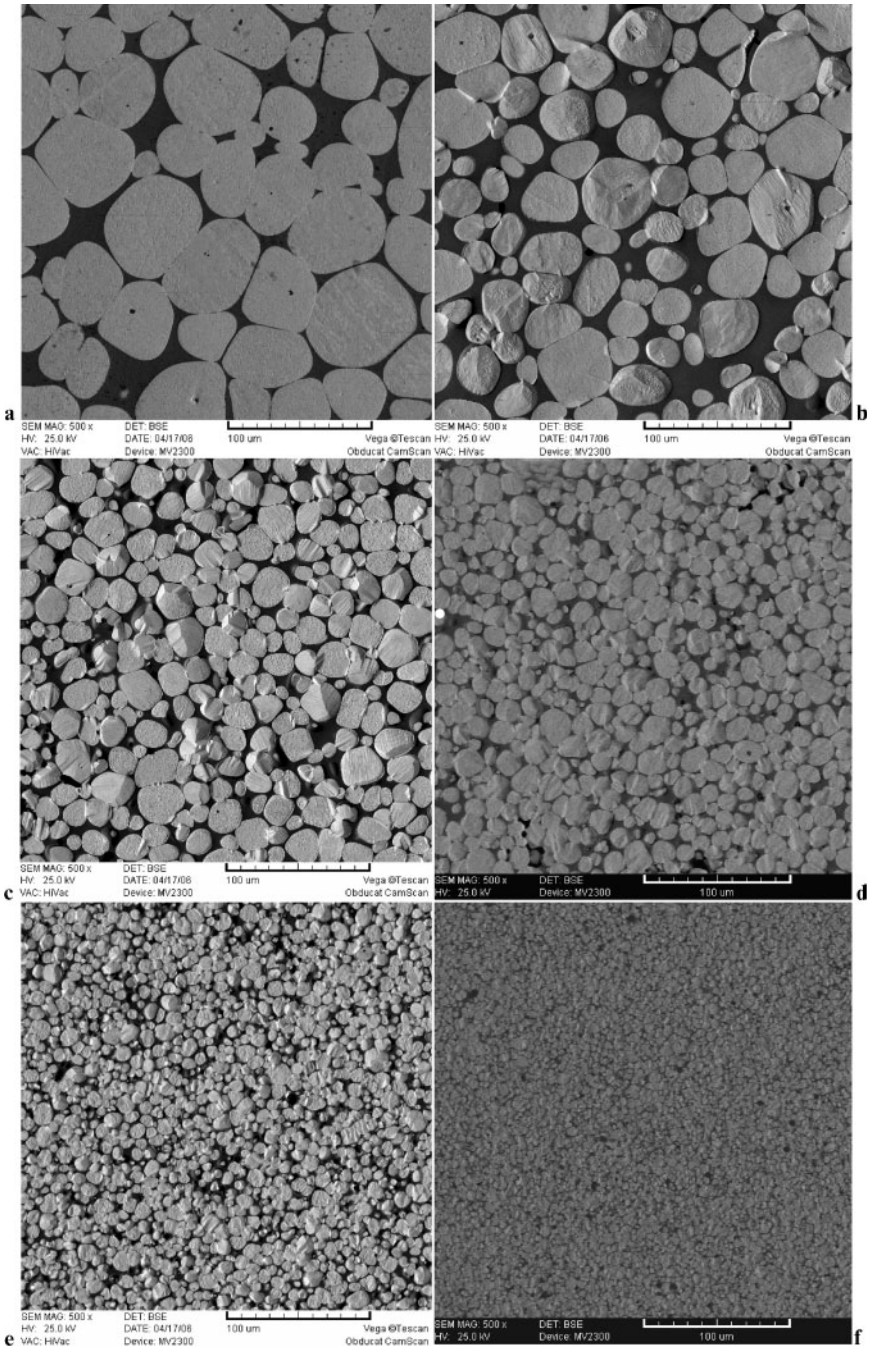

8 Microstructure of samples having 90 (wt-%)W but different Mn/Ni ratio *a* 1/9; *b* 2/8; *c* 4/6; *d* 5/5; *e* 6/4; *f* 8/2

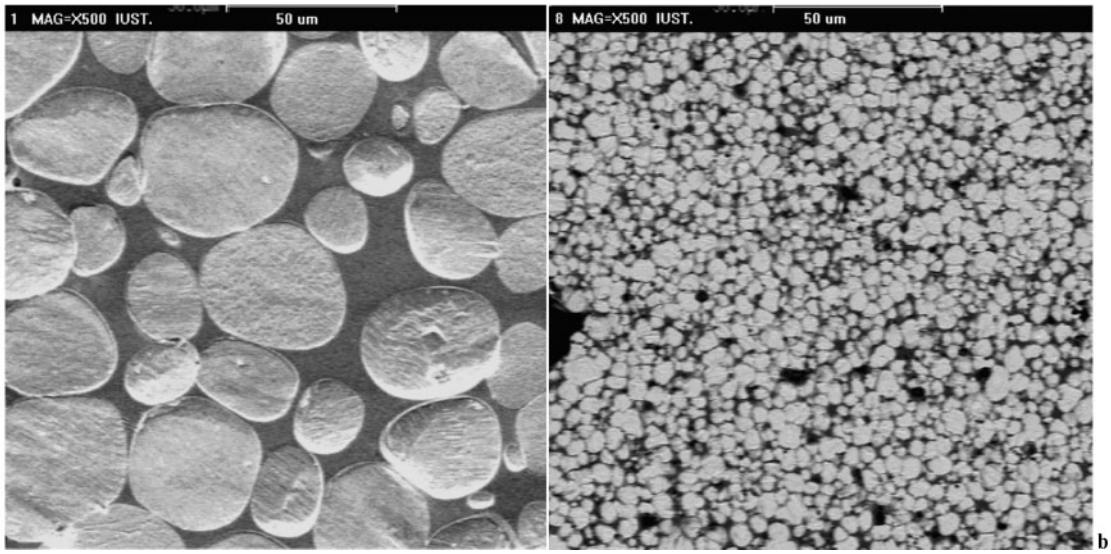

9 Characteristics of W particles within *a* 90W–9Ni–Mn and *b* 90W–2Ni–8Mn alloys

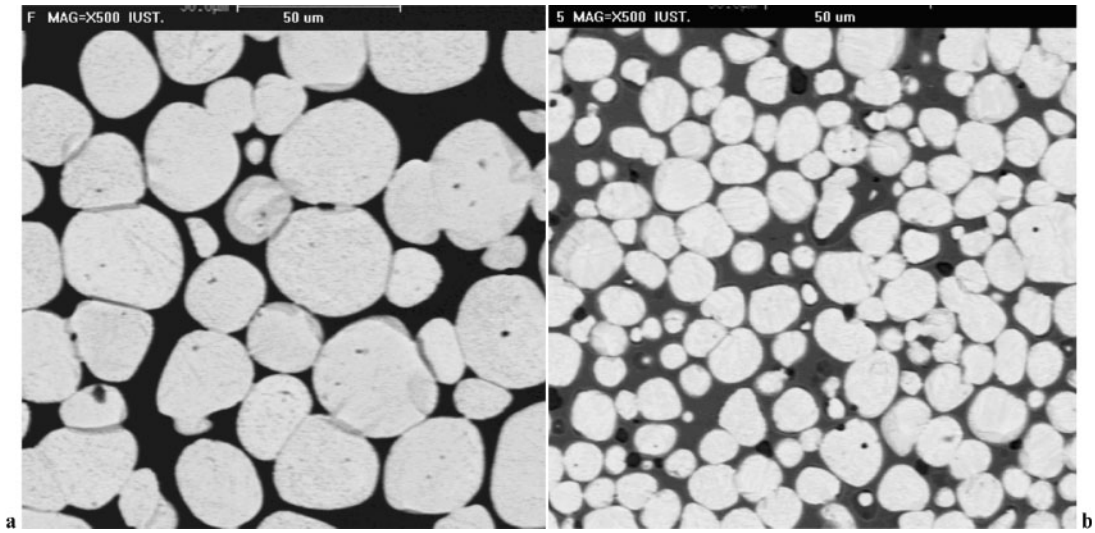

10 Microstructure of *a* 90W–7Ni–3Fe and *b* 90W–7Ni–3Mn alloys

If the mean size of W particles within 7Ni–3Fe matrix (i.e. 50 μm) is considered and compared with that obtained in this research (i.e. 27 μm) for 7Ni–3Mn matrix, it may be concluded that the growth of W grains within the Ni–Fe matrix was more than that of Ni–Mn matrix. Thus, the above argument about the lower rate of growth of W particles within Ni–Mn matrix seems logical.

The shape of W particles within Ni–Fe matrix was more spherical than W particles within Ni–Mn matrix. W particles within Ni–Mn matrix had sharper edges than those in Ni–Fe matrix due to lower dissolution of W in Mn–Ni matrix. Therefore, it seems due to higher solubility of W particles within the Ni–Fe matrix in comparison with Ni–Mn matrix, the amount of tungsten dissolves in Ni–Fe which causes reprecipitation of more tungsten on the exited W particles within Ni–Fe matrix, especially at high temperature or at longer sintering time.[19,20]

Conclusions

Effects of different Mn/Ni ratios in the microstructure of W heavy alloys have been studied and the following conclusions are obtained.

1. As Mn/Ni ratio increased, tungsten solubility in the matrix decreased due to the presence of Mn in matrix and insolubility of tungsten in Mn.
2. The presence of Mn in this type of alloys caused refinement of W grains.
3. As the Mn/Ni ratio increased the sharp edges of polygonal W grain became less rounded.
4. It was confirmed that tungsten has less solubility in Ni–Mn matrix compared to a Ni–Fe matrix at an equivalent ratio of Fe/Ni and Mn/Ni.

Acknowledgement

Special thanks go to Khorasan Metallurgy Industry for their financial support.

References

1. R. M. German: 'Liquid phase sintering', 223–236; 1985, New York, Plenum Press.
2. A. Upadhyaya: *Mater. Chem. Phys.*, 2001, **67**, 101–110.
3. A. Bleise, P. R. Danesi and W. Burkart: *J. Environ. Radioactiv.*, 2003, **64**, 93–112.
4. R. Pöllänen, T. K. Ikaheimonen and S. Klemola, *et al.*: *J. Environ. Radioactiv.*, 2003, **64**, 133–142.

5. C. Giannardi and D. Dominici: *J. Environ. Radioactiv.*, 2003, **64**, 227–236.
6. D. E. McClain, K. A. Benson, T. K. Dalton, J. Ejnik, C. A. Emond, S. J. Hodge, J. F. Kalinich, M. A. Landauer, A. C. Miller, T. C. Pellmar, M. D. Stewart, V. Villa and J. Xu: *Sci. Total Environ.*, 2001, **274**, 115–118.
7. J. P. McLavghlin, L. Leon Vintro and K. J. Smith, *et al.*: *J. Environ. Radioactiv.*, 2003, **64**, 155–165.
8. D. K. Kim, S. Lee and W. H. Baek: *Mater. Sci. Eng. A*, 1998, **A249**, 97–205.
9. L. S. Magness, Jr: Proc. 1st Int. Conf. on 'Tungsten and tungsten alloys', Princeton, NJ, USA, 1992, MPIF, 15–22.
10. R. M. German and A. Bose: *Met. Powder Rep.*, 1992, **47**, (11), 42–46.
11. M. N. Bassim: *J. Mater. Process. Technol.*, 2001, **119**, 234–236.
12. A. Bose, H. Couque and J. Lankford, Jr: Proc. 1st Int. Conf. on 'Tungsten and tungsten alloys', Princeton, NJ, USA, 1992, MPIF, 291–298.
13. M. H. Hong: US Patent 5970307, October 1999.
14. A. Bose, S. C. Yang and R. M. German: *Adv. P/M*, 1991, **6**, 425–437.
15. T. B. Mussalski (ed.): 'Binary alloy phase diagrams'; 1986, Metals Park, OH, ASM.
16. R. M. German: 'Sintering theory and practice', 438–444; 1996, New York, John Wiley & Sons.
17. I. M. Lifshitz and V. V. Slyozov: *J. Phys. Chem. Solid.*, 1961, **19**, 35–50.
18. R. M. German: *Prog. P/M*, 1986, 235–247.
19. H. Riegger, J. A. Pask and H. E. Exner: *Mater. Sci. Res.*, 1979, **13**, 219–233.
20. R. M. German, A. Bose and S. S. Mani: *Mater. Trans. A*, 1992, **23A**, 211–219.